

Ultrafast Structural Deformation of Polyatomic Molecules in Intense Laser Fields

Kaoru Yamanouchi,* Akiyoshi Hishikawa, Atsushi Iwamae, and Shilin Liu

*Department of Chemistry, School of Science, The University of Tokyo
7-3-1 Hongo, Bunkyo-ku, Tokyo 113-0033, Japan*

Abstract. The momentum vector distributions of fragment ions produced through the Coulomb explosion of small molecules such as NO, CO₂, NO₂, and H₂O in intense laser fields (~1 PW/cm²) are measured by the mass-resolved momentum imaging (MRMI) technique. For NO, the MRMI maps for a single (*p*,*q*) pathway, NO(*p+q*)⁺ → N^{*p*+} + O^{*q*+} (*p*, *q* = 1~3), are extracted from the observed MRMI maps on the basis of the momentum matching of the N^{*p*+} and O^{*q*+} ion pair. In the MRMI maps for the fragment ions produced from CO₂, NO₂, and H₂O, their ultrafast structural deformation both along the stretching coordinate and along the bending coordinate is identified. The ∠O-C-O angle distribution of CO₂ spreads significantly (FWHM ~40°), and the ∠O-N-O bond angle of NO₂ increases toward a linear configuration within the ultrashort duration of the laser pulse. This type of deformation is also identified for H₂O. These structural deformations are most reasonably interpreted as a consequence of the formation of *light-dressed* potential energy surfaces.

INTRODUCTION

One of the characteristic features of ultrashort laser pulses is their capability of generating an extremely intense light field. It is now possible to increase the magnitude of the laser field as large as a Coulombic electric field in a hydrogen atom. In such an intense laser field, *light-dressed* potential energy surfaces (LDPESSs) are formed by the interaction among the molecular potentials shifted by an energy of photons.¹ Therefore, nuclear dynamics of molecules is expected to be governed by LDPESSs, which have been investigated intensively for one electron system of H₂⁺. Recent studies of molecules which have more than one electrons demonstrated that a variety of fundamental dynamics are associated with the formation of LDPESSs in intense laser fields.²⁻⁸

When molecules are irradiated by the intense laser light whose magnitude is comparable with the valence electric-field in atoms and molecules, the phenomenon called the Coulomb explosion occurs, in which multiply charged atomic fragments having a large released momentum are produced.¹⁻¹² The molecular Coulomb

CP500, *The Physics of Electronic and Atomic Collisions*, edited by Y. Itikawa, et al.
© 2000 American Institute of Physics 1-56396-777-4/00/\$17.00

explosion in intense laser fields is known to exhibit two characteristic features, i.e. (i) ultrafast geometrical deformation occurring during the short laser-pulse duration, and (ii) anisotropic ejection of the atomic and molecular fragment ions representing the alignment of the parent molecular ions with respect to the laser polarization direction.

Recently, in order to investigate the ultrafast nuclear dynamics of molecules in intense laser fields, we introduced a novel method called mass-resolved momentum imaging (MRMI).²⁻⁸ In the MRMI method, atomic and molecular fragment ions ejected with a large released momentum are detected by a time-of-flight (TOF) mass spectrometer, and the momentum as well as angular distributions of the ejected ion species are obtained by rotating the direction of the laser polarization with respect to the detection axis of the TOF tube. Due to the high resolving power of our TOF mass spectrometer, atomic and molecular ions with different charge numbers are observed separately. The resultant momentum and angular distributions of the charged species are plotted either on the two-dimensional (2D) momentum plane as a contour map or in the form of three-dimensional (3D) intensity distribution on the momentum plane. By the analysis of the imaging maps, it becomes possible to extract geometrical structure of molecules just before the Coulomb explosion, from which we discuss the ultrafast geometrical deformation occurring within an intense laser pulse.

In the present study, by referring to our recent studies of ultrashort dynamics of diatomic^{2,3} and triatomic^{2,6-8} molecules in intense laser fields using the MRMI approach, we report how the deformation of their geometrical structure occurs and how these phenomena are interpreted in terms of the formation of LDPESSs.

EXPERIMENT

The details of our experimental set-up were presented previously.²⁻⁸ Briefly, femtosecond laser pulses at $\lambda \sim 800$ nm generated by a mode-locked Ti-sapphire laser (Spectra Physics Tsunami + Millennia) were introduced into a regenerative amplifier system (BM Industry Alpha 10B/S) to obtain high-power short-pulsed laser light at a repetition rate of 10 Hz. After a pulse compression, a laser-pulse duration of 100 fs was achieved with a total energy of up to 50 mJ/pulse.

The laser beam was focused by a quartz lens onto a skimmed pulsed molecular beam of a sample gas in the region between the extraction parallel repeller plates of a linear TOF mass spectrometer.

In our TOF mass spectrum with typical mass resolution of $m/\Delta m \sim 620$, ion species with different charge numbers were resolved well with no temporal overlap. The TOF mass spectrum with a high S/N ratio was obtained by accumulating the spectra for $\sim 1 \times 10^3$ laser shots using a digital oscilloscope (LeCroy 9370) at a 1 GHz sampling rate. When the pulsed valve was not operated, the background pressure in the main chamber was 2×10^{-8} Torr and that in the TOF tube was 1×10^{-8} Torr. During the

experiment, the pressure in the main chamber was kept sufficiently low ($< 2 \times 10^{-7}$ Torr) in order to avoid the space charge effect.

For constructing the MRMI maps, the TOF mass spectra were taken at different laser polarization angles by rotating the laser polarization using a zero-order half-wave plate, which was introduced after the pulse compression stage of the regenerative amplification system. The half-wave plate was rotated manually or automatically with a small angle interval of $\sim 6^\circ$.

MRMI AND SP-MRMI MAPS: APPLICATION TO NO

The momentum-scaled (MS) TOF spectra were measured for the atomic fragment ions, N^{p+} and O^{q+} ($p, q = 1-3$), produced in the intense laser field ($\sim 1.4 \text{ PW/cm}^2$) from the (p, q) Coulomb explosion pathways of NO, i.e. $\text{NO}^{z+} \rightarrow N^{p+} + O^{q+}$ ($z = p+q$), and they were used to construct mass-resolved momentum imaging (MRMI) maps.⁵

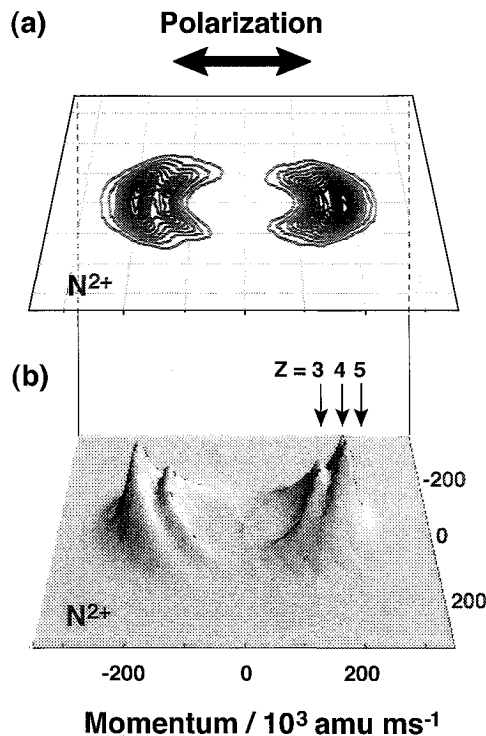
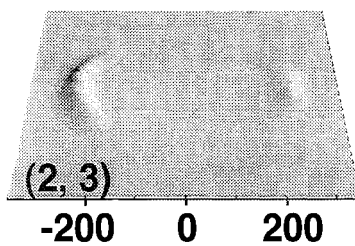
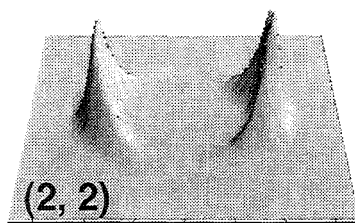
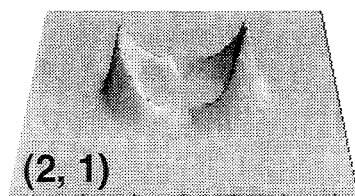
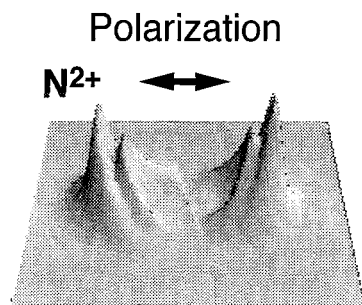


FIGURE 1. The 2D (upper) and 3D (lower) MRMI maps of N^{2+} produced via the Coulomb explosion of NO^{z+} ($z = 3 - 5$) formed in intense laser fields.



Momentum / 10^3 amu ms⁻¹

FIGURE 2. The observed MRMI map of N^{2+} produced via the Coulomb explosion of NO^{2+} in intense laser fields and its decomposition into the SP-MRMI maps for the $(p, q) = (2,1)$, $(2,2)$, and $(2,3)$ pathways.

Figure 1 shows the 2D and 3D MRMI maps of the N^{2+} channel formed through the $(p,q) = (2,1), (2,2),$ and $(2,3)$ explosion pathways from the parent NO^{z+} ions with the total charges of $z = 3, 4,$ and $5,$ respectively.

In order to extract momentum and angular distributions for the respective (p,q) Coulomb explosion pathways from the obtained MRMI maps, the least-squares fits using the Gaussian momentum distribution functions were performed for all the MS-TOF spectra obtained at the different laser-polarization angles, and the resultant Gaussian distributions for each (p,q) pathway were transformed into the corresponding single-pathway (SP)-MRMI map.

In Fig. 2, the extraction of the SP-MRMI maps from the observed MRMI map is shown in the 3D representation for the N^{2+} channel formed from NO^{z+} . It is clearly seen that the observed MRMI map is decomposed into the three MRMI maps representing the $(2,1), (2,2),$ and $(2,3)$ pathways, and that the narrower angular distributions for the (p,q) explosion pathways were derived for a larger total charge z of NO^{z+} .

SPREAD OF BOND ANGLE DISTRIBUTION IN CO_2

The upper panels of Fig. 3 show the observed MRMI maps for the fragment atomic ions, C^{q+} ($q = 2, 3$), produced after the (p, q, r) Coulomb explosion of CO_2 , i.e., $CO_2^{z+} \rightarrow O^{p+} + C^{q+} + O^{r+}$ ($z = p+q+r$), at the field intensity of $1.1 \text{ PW} / \text{cm}^2$.⁶ These C^{q+} ($q = 2, 3$) channels have an elliptical pattern substantially extending perpendicular to the laser polarization with a peak at the zero momentum. This shows that the C^{2+} and C^{3+} ions gain only small released momenta even though they are formed from the highly charged parent ions, and that they are ejected more preferentially in the direction perpendicular to the laser polarization vector.

In order to derive quantitative information concerning the structure of CO_2^{z+} prior to the dissociation, we performed a trial-and-error simulation of the MRMI maps of all the atomic fragment ions by taking the following steps: (i) the released momenta of fragment ions for a given molecular geometry are calculated, and they are converted into the MRMI maps for a single (p, q, r) explosion pathway by taking account of the distributions of $R = R(C-O)$ and $\gamma = \angle O-C-O$, (ii) the MRMI map for a given fragment ion is synthesized by adding the relevant SP-MRMI maps with their weights estimated from the observed yields of O^{p+} , and (iii) the geometrical parameters R and γ are determined as a function of z on the basis of the trial-and-error comparison of the synthesized and observed MRMI maps for all the fragment ions.

The bond length $R(C-O)$ determined through the analysis of the MRMI maps of all the atomic fragment ions exhibits a gradual increase as z increases, which is consistent with the recent studies of diatomic molecules, N_2 and NO , and triatomic molecules, NO_2 and H_2O in an intense laser fields.

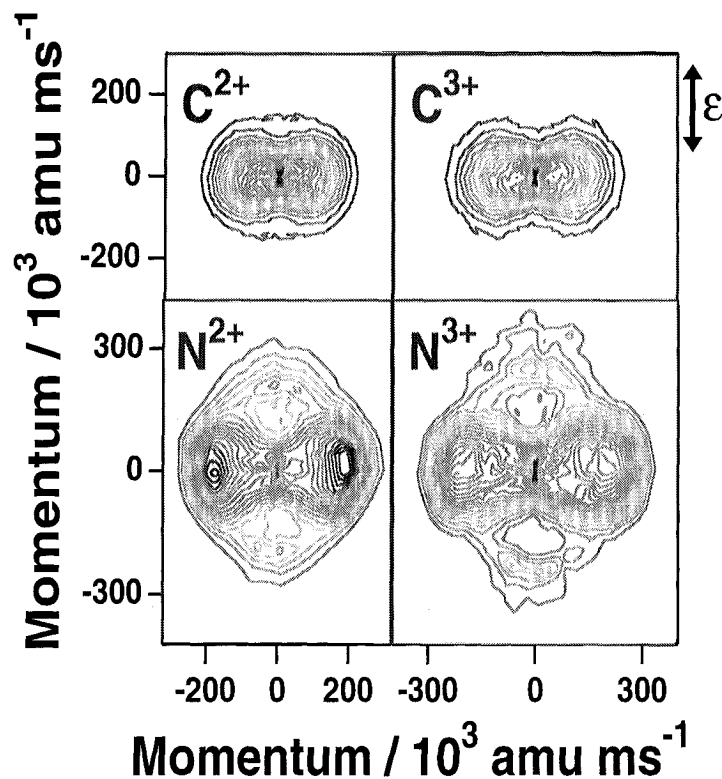


FIGURE 3. The MRMI maps of C^{2+} and C^{3+} formed from CO_2 (upper panels) and those of N^{2+} and N^{3+} formed from NO_2 (lower panels) in intense laser fields. The direction of the laser polarization vector, ϵ , is represented by a vertical arrow.

It was also found that the Gaussian width σ_γ of the bond angle distribution becomes $\sigma_\gamma = 50 \sim 30^\circ$ for $z = 3 \sim 9$. Considering the mean amplitude of bending, $\sigma_\gamma = 12.5^\circ$, in the ground vibrational level of the $\bar{X}^1\Sigma_g^+$ state of neutral CO_2 , the present results clearly show that a substantially broad γ distribution centered at the linear configuration is induced in the intense laser field. The present observation is in agreement with the report by Cornaggia,⁹ who assumed a simple triangular γ distribution and derived its FWHM to be 40° for $z = 3 - 6$.

The observed broad γ distributions would be ascribed to the laser-induced population transfer to an excited state having a bent equilibrium; i.e., the linear ground and the excited bent state are coupled strongly by the intense laser field to form a significant avoided crossing resulting in a pair of adiabatic LDPEs (Fig.4). It is

expected that the potential barriers of the lower component of the resultant adiabatic LDPEs along the bond-angle coordinate are lowered at a high field intensity to cause potential softening along the bond-angle coordinate, which causes the ultrafast nuclear motion toward the bent structure within a laser-pulse duration.

BENT-TO-LINEAR DEFORMATION OF NO₂

The lower panels of Fig. 3 show the observed MRMI maps for the fragment atomic ions, N^{q+} ($q = 2, 3$), produced after the three-body (p, q, r) Coulomb explosion of NO₂, i.e., NO₂^{z+} → O^{p+} + N^{q+} + O^{r+}, at the field intensity of 1.0 PW/cm².⁷ Both the N²⁺ and N³⁺ channels have a substantially elongated pattern with two peaks at large released momenta ($\sim 200 \times 10^3$ amu m/s) in the perpendicular direction to the laser polarization. The characteristic fragmentation patterns exhibit a contrast with those observed for C^{q+} ($q = 2, 3$) ions formed from CO₂ shown in the upper panels in Fig. 3, where elliptical distributions with a peak at the zero momentum were observed.

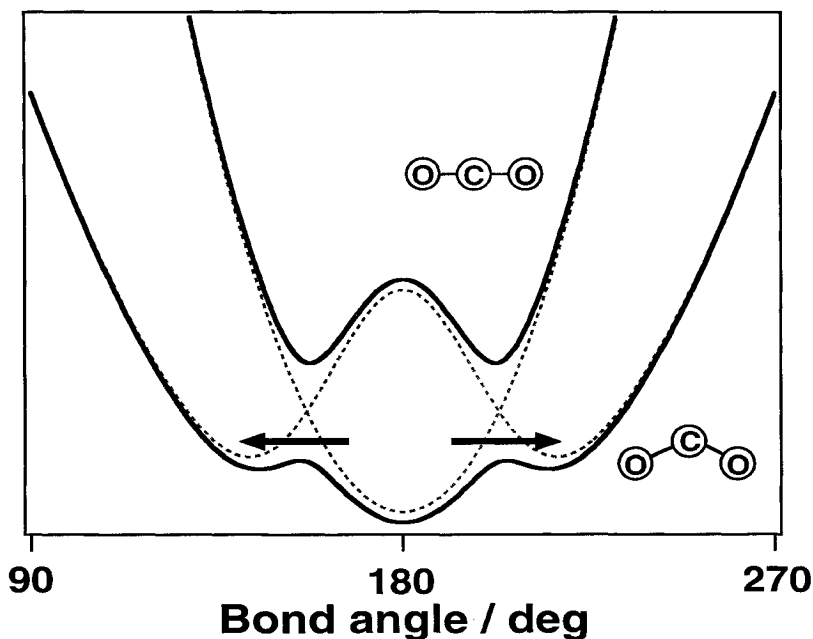


FIGURE 4. A schematic diagram of the formation of the *light-dressed* potential energy surfaces of CO₂ in intense laser fields (one dimensional cut along the bending coordinate).

The large momentum imposed on N^{q+} ($q = 2, 3$) along the perpendicular direction of the polarization vector suggests that the NO_2^{z+} ions take a bent skeletal geometry just before the three-body explosion processes with its a-axis along the laser polarization vector.

A closer inspection of the MRMI map of N^{2+} reveals that the momentum distribution extends substantially along the coordinate perpendicular to the laser polarization (horizontal coordinate) toward the center of the map from the peaks at $\sim 200 \times 10^3$ amu m/s. The distribution at the zero momentum reaches about a half as large as that for the two peaks.

If symmetric charge separation pathways are assumed, the zero released-momentum imposed on the central atom results exclusively from the linear geometry of the parent molecular ion. Therefore, the present finding suggests that the probability distribution in the linear geometrical configuration substantially increases from the original equilibrium bent structure of the ground state of NO_2 ($\gamma_e = 134.1^\circ$).

The substantial increase in the probability distribution at the linear configuration is more clearly seen in the MRMI map of N^{3+} shown in Fig. 3, where the momentum distribution is almost flat along the horizontal axis with the highest peak located at the zero momentum region. The observed momentum distribution of N^{q+} ($q = 2, 3$) in Fig. 3 could be regarded as a direct evidence for a substantial deformation of NO_2 induced by the intense laser field not only along the stretching coordinate but also along the bending coordinate.

In order to derive more quantitative information, we performed a trial-and-error simulation of the MRMI maps of all the atomic fragment ions in a similar manner as in the case of CO_2 . For the simplification of the analysis, we modeled the mean bond angle as a linear function of the charge z , i.e., $\gamma_0(z) = c_0 + c_1 z$, where c_0 and c_1 are constants. As the optimized parameters, $c_0 = 105^\circ$ and $c_1 = 8.33$, were obtained from the MRMI map of N^{2+} . The best fit MRMI map for N^{2+} reproduces well the observed map in the entire momentum region. It was also found that the same $\gamma_0(z)$ function provides a good fit for N^{3+} .

Three low lying excited states, \tilde{A}^2B_2 , \tilde{B}^2B_1 , \tilde{C}^2A_2 , of NO_2 are accessible from the ground \tilde{X}^2A_1 state through one- or two-photon absorption of near-IR light used in the present study. Since the photon-molecule interaction is most effective for a pair of electronic states coupled with a single photon transition, the one-photon light-induced coupling between the \tilde{X}^2A_1 and \tilde{A}^2B_2 states would dominate over the other higher-order photon-molecule interactions, resulting in the formation of the LDPEs through the avoided-crossing between these two low-lying electronic states. Since the equilibrium bond angles of the \tilde{X}^2A_1 and \tilde{A}^2B_2 states are $\gamma_e = 134^\circ$ and 102° , respectively, the lower component of the pair of the LDPEs would provide force to bent NO_2 from $\gamma_e = 134^\circ$ to a smaller bond angle. The significantly small bond-angle $\gamma_0(z=0) = c_0 = 105^\circ$ derived from the simulation could be regarded as an evidence of the formation of the LDPEs between the \tilde{X}^2A_1 and \tilde{A}^2B_2 states.

At higher laser-field intensities, the two-photon vibronic transition from \tilde{X}^2A_1 to

\tilde{B}^2B_1 would become important. Since the \tilde{B}^2B_1 state has a linear equilibrium structure, i.e., $\gamma = 180^\circ$, the lower component of the two LDPEs formed by the mixing of the \tilde{X}^2A_1 and \tilde{B}^2B_1 would drive the originally bent NO_2 toward the linear configuration.

EXPLOSION DYNAMICS OF H_2O

The MRMI maps of H^+ , O^+ and O^{2+} produced through the Coulomb explosion of H_2O in the intense laser field were measured using the ultrashort laser pulses with wavelength of $\lambda \sim 800$ and 400 nm.⁸ For both wavelengths, the two Coulomb explosion processes of H_2O , i.e., (i) $\text{H}_2\text{O}^{3+} \rightarrow \text{H}^+ + \text{O}^+ + \text{H}^+$ and (ii) $\text{H}_2\text{O}^{4+} \rightarrow \text{H}^+ + \text{O}^{2+} + \text{H}^+$ were clearly identified.

The MRMI maps show that the H^+ ions are ejected mainly in the direction parallel with the laser polarization vector. As an example, the MRMI map of H^+ observed when $\lambda \sim 400$ nm is shown in Fig. 5. From the analysis of the MRMI patterns of the fragment ions, the geometrical structure of H_2O^{3+} and H_2O^{4+} just before the Coulomb explosion as well as the extent of their alignment along the laser polarization vector were obtained.

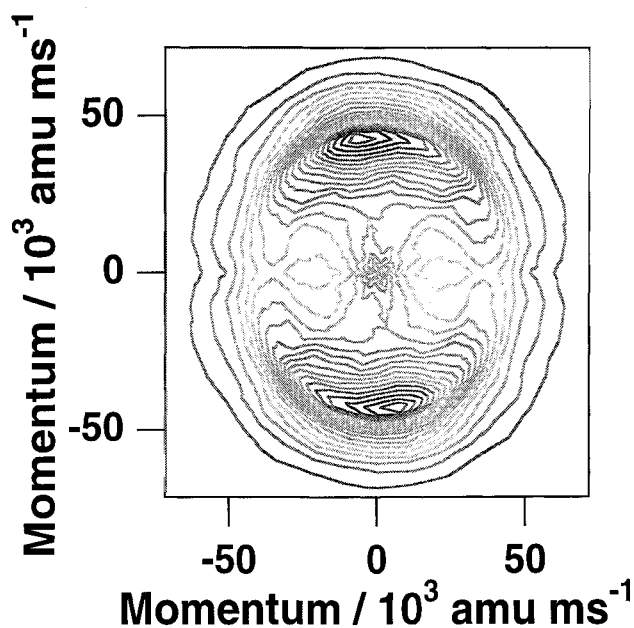


FIGURE 5. The observed MRMI map of H^+ produced from the Coulomb explosion of H_2O in intense laser fields of $\lambda \sim 400$ nm.

In a similar manner as the analyses of the MRMI maps described above for CO₂ and NO₂, the measured MRMI maps of H⁺, O⁺, and O²⁺ ions were simulated to reproduce their momentum distributions simultaneously. When light pulses of $\lambda \sim 800$ nm are used, it was shown from the trial-and-error simulation that (i) the O-H bond lengths of H₂O³⁺ and H₂O⁴⁺ just before the Coulomb explosion are respectively 1.7 and 2.0 times longer than that of the neutral H₂O in the electronic ground state, and (ii) the bond angle $\gamma (= \angle \text{H-O-H}) \sim 180^\circ$ and its distribution width is $\sigma_\gamma = 60^\circ$ for both parent ions. This bond-angle widening from that of neutral H₂O ($\gamma = 104.45^\circ$) could also be interpreted as a phenomenon caused by the ultrafast geometrical deformation of H₂O⁺ on the *light-dressed* potential energy surface.¹³

ACKNOWLEDGEMENTS

The authors thank Drs. K. Hoshina and M. Kono for their valuable discussion and assistance in the experiments. The present work has been supported by the CREST (Core Research for Evolutionary Science and Technology) fund from Japan Science and Technology Corporation.

REFERENCES

1. Bandrauk, A. D., *Molecules in Intense Laser Fields*, New York: M. Dekker Pub., 1993.
2. Hishikawa, A., Iwamae, A., Hoshina, K., Kono, M., and Yamanouchi, K., *Chem. Phys. Lett.* **282**, 283 (1998).
3. Hishikawa, A., Iwamae, A., Hoshina, K., Kono, M., and Yamanouchi, K., *Chem. Phys.* **231**, 315 (1998).
4. Hishikawa, A., Iwamae, A., Hoshina, K., Kono, M., and Yamanouchi, K., *Res. Chem. Intermed.* **24**, 765 (1998).
5. Iwamae, A., Hishikawa, A., and Yamanouchi, K., *submitted to J. Phys. B*.
6. Hishikawa, A., Iwamae, A., and Yamanouchi, K., *Phys. Rev. Lett.* **83**, 1127 (1999).
7. Hishikawa, A., Iwamae, A., and Yamanouchi, K., *J. Chem. Phys.* **111** (1999), *in press*.
8. Liu, S., Hishikawa, A., Iwamae, A., and Yamanouchi, K., unpublished.
9. Cornaggia, C., Normand, D., and Morellec, J., *J. Phys. B: At. Mol. Opt.* **25** 415 (1992).
10. Posthumus, J. H., Plumridge, J., Taday, P. F., Sanderson, J. H., Langley, A. J., Codling, K., and Bryan, W. A., *J. Phys. B: At. Mol. Opt.* **32** L93 (1999).
11. Sanderson, J. H., El-Zein, A., Bryan, W. A., Newell, W. R., Langley, A. J., and Taday, P. F., *Phys. Rev. A* **59**, R2567 (1999).
12. Constant, E., Stapelfelt, H., and Corkum, P. B., *Phys. Rev. Lett.* **76**, 4140 (1996).
13. Rottke, H., Trump, C., and Sandner, W., *J. Phys. B: At. Mol. Opt.* **31**, 1083 (1998).